

Investigation of impurity transport and radiation characteristics in SlimCS DEMO reactor by the divertor simulation code SONIC

ダイバータシミュレーションコードSONICによる原型炉SlimCSにおける不純物輸送と放射損失特性の検討

Asakura Nobuyuki¹⁾, Shimizu Katsuhiko²⁾, Hoshino Kazemasa¹⁾, Tobita Kenji¹⁾, Takizuka Tomonori²⁾
朝倉 伸幸¹⁾、清水 勝宏²⁾、星野 一生¹⁾、飛田 健次¹⁾、滝塚 知典²⁾

Japan Atomic Energy Agency

1) 2-166 Omotedate, Obuchi, Rokkasho, Kamikita-gun, Aomori 039-3212, Japan

2) 801-1 Mukoyama, Naka, Ibaraki 311-0193, Japan

日本原子力研究開発機構

1) 〒039-3212 青森県上北郡六ヶ所村尾駮表館2-166

2) 〒311-0193 茨城県那珂市向山801-1

Power handling for the demo tokamak reactor, SlimCS, with the exhausted power of $P_{\text{out}} = 500$ MW and intense Ar impurity seeding was investigated, using SONIC code, where impurity transport is simulated by Monte Carlo calculation (IMPMC). In the radiative and detached divertor, Ar density and its concentration were increased upstream the divertor target. Impurity distribution in the divertor and the influence on the power load profile were summarized. At the same time, results are compared with the SOLDOR/NEUT2D simulation using a non-coronal equilibrium and assuming Ar concentration (n_{Ar}/n_i).

1. Introduction

Handling of a large exhausted power from the core plasma is the most important issue for the fusion reactor design, which requires control of edge and divertor plasmas as well as development of the plasma facing components. Exhausted power to the edge and SOL (P_{out}) becomes large such as several 100 MW compared to that in ITER (about 100 MW). For the development of the plasma operation scenario and divertor design, the total radiation loss fraction ($f_{\text{rad}}^{\text{tot}} = P_{\text{rad}}^{\text{tot}}/P_{\text{out}}$, $P_{\text{rad}}^{\text{tot}}$ is the total radiation power at the divertor, SOL and edge) of more than 90 % is required.

Divertor design for the power handling in the tokamak demo reactor, SlimCS [1], has recently progressed [2], using the integrated divertor code, SONIC [3-4]. Ar gas seeding was used to increase the radiation loss power, and effect of the divertor geometry on the heat and particle fluxes was enhanced from the design concept for ITER in order to reduce the peak heat load. Under the radiative and detached divertor condition, the heat load profile is determined mostly by distribution of the radiation loss from impurity ions rather than that by the plasma transport. Therefore, investigation of the impurity transport becomes more important to determine the power handling in the DEMO divertor.

Monte Carlo code (IMPMC) has advantages for impurity modelling since most kinetic effects on the impurity ions such as thermal and friction forces along the magnetic field are incorporated in original

formula. In this study, the impurity transport and the radiation loss distribution in the divertor are investigated, comparing with an evaluation of the simple radiation model, where non-coronal equilibrium (radiation power function) [4] is used and a constant value of Ar impurity concentration (n_{Ar}/n_i) is given over the divertor region.

2. Radiation and heat load in SlimCS divertor

SlimCS is a conceptual DEMO design of a low aspect ratio tokamak ($R/a = 2.6$ with a reduced-size Central Solenoid coils) with the core dimension similar to those in ITER and power generation capability of a giga-watt level [1]. SONIC calculation has been performed with injecting Ar gas at two locations (one at the outer SOL and another from the outer divertor) and determining the Ar puff rate to obtain a given $P_{\text{rad}}^{\text{tot}}$. Here, core plasma boundary ("edge") for the calculation is set at $r/a = 0.95$, where $P_{\text{out}} = 500$ MW and the total ion flux of $\Gamma_{\text{out}} = 5 \times 10^{22}$ D/s are exhausted. Gas puff of $\Gamma_{\text{puff}} = 1 \times 10^{23}$ D/s (~ 200 Pa·m³/s) is injected at the outer divertor throat.

Peak heat load at the divertor target, q_{target} , is evaluated, including heat load due to radiation power (F_r) and neutral flux (F_n), by,

$$q_{\text{target}} = \gamma \cdot n_d C_{sd} T_d + n_d C_{sd} E_{\text{ion}} + F_r(P_{\text{rad}}) + F_n(\frac{1}{2} m_0 v_0^2 \cdot n_0 v_0), \quad (1)$$

where γ , n_d , C_{sd} , T_d , E_{ion} are sheath transmission coefficient, density, plasma sonic speed,

temperature at the divertor sheath, and surface recombination energy, respectively. The first and second terms in RHS correspond to the total heat load transported by the plasma convection and conduction (“transport component”), and the surface recombination energy of the low temperature ions, respectively. The third and fourth terms are the radiation loading and neutral flux (due to charge exchange and volume recombination), respectively, which become dominant in the radiative and detached divertor.

Profiles of the heat load components at the outer divertor for the case of $P_{\text{rad}}^{\text{tot}} = 460$ MW ($f_{\text{rad}}^{\text{tot}} = 0.92$) are shown in Fig. 1. In a steady-state solution, the radiation distribution at the edge, SOL and divertor is determined mostly by the Ar ion transport rather than the gas puff location. The radiation loss power at the edge and SOL ($P_{\text{rad}}^{\text{Edge\&SOL}}$) is 195 MW ($f_{\text{rad}}^{\text{Edge\&SOL}} = 0.39$), thus power flow of 305 MW is exhausted into the divertor. In the divertor, $P_{\text{rad}}^{\text{in-div}} = 114$ MW ($f_{\text{rad}}^{\text{in-div}} = 0.23$) and $P_{\text{rad}}^{\text{out-div}} = 151$ MW ($f_{\text{rad}}^{\text{out-div}} = 0.30$), and peak heat load at the outer target ($q_{\text{target}}^{\text{out}}$) of 14.2 MWm⁻² is observed at 7 cm outer from the strike-point. The transport component is decreased to 3.2 MWm⁻² and the surface recombination is 4.1 MWm⁻² while the radiation power load becomes the dominant component of 6.7 MWm⁻². Therefore, control of the impurity distribution in the divertor plasma becomes important as well as the divertor detachment.

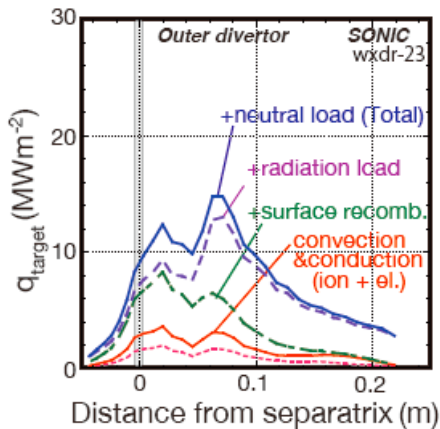


Fig.1 Profiles of total heat load at the outer target and the components: electron and ion transport (convection and conduction) fluxes, surface recombination energy, radiation power load, and neutral flux, for the case of $P_{\text{rad}}^{\text{tot}} = 460$ MW.

3. Comparison with a simple radiation model

A simple radiation model with non-coronal equilibrium [5] and assuming a constant ratio of

impurity density to ion density, n_{Ar}/n_i , was used in the calculation of the plasma fluid code (SOLDOR) and neutral Monte Carlo code (NEUT2D), which has an advantage to reduce the calculation time to obtain a solution. Two components of the target power loading, i.e. transport and radiation (plus neutral flux and surface recombination) components, are shown as Case-1, -2 and -3 in Fig. 2. Here, n_{Ar}/n_i at the outer divertor is increased from 2% (Case-2) to 5% (Case-3) [6], where the divertor geometry with the V-shaped corner at the bottom of the outer divertor, and $n_{\text{Ar}}/n_i = 1\%$ in the inner divertor and edge regions are the same. $P_{\text{rad}}^{\text{Edge\&SOL}} = 138$ MW and power to the divertor is 362 MW.

For the Case-3 ($n_{\text{Ar}}/n_i = 5\%$), $P_{\text{rad}}^{\text{out-div}}$ is significantly increased to 238 MW ($f_{\text{rad}}^{\text{out-div}} = 0.48$) and $P_{\text{rad}}^{\text{tot}} = 493$ MW ($f_{\text{rad}}^{\text{tot}} = 0.98$). The total $q_{\text{target}}^{\text{out}}$ is reduced to 9.2 MWm⁻², where the transport and radiation components are 2.1 and 4.6 MWm⁻², respectively. Two results of SONIC results (larger symbols) with increasing the Ar seeding rate are compared with the simple radiation model in Fig. 2. The radiation component considering the impurity transport becomes larger, thus the impurity radiation is localized just above the target. Kinetic effects on the impurity transport and radiation distribution in the DEMO divertor are discussed.

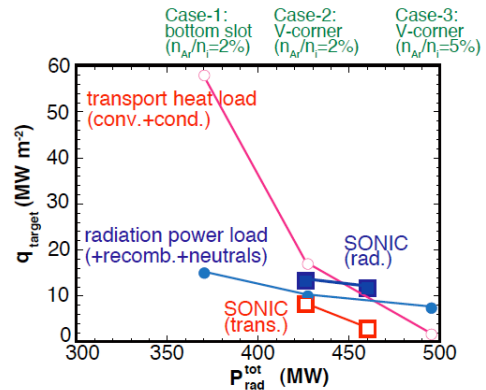


Fig.2 Two components (transport and radiation power) of peak heat flux at the outer target as a function of total radiation power, $P_{\text{rad}}^{\text{tot}}$, for the simple radiation model (Case-1, Case-2, Case-3: small symbols) and SONIC results (large symbols).

References

- [1] K. Tobita *et al.*: Nucl. Fusion **49** (2009) 075029.
- [2] N. Asakura, *et al.*: J. Plasma Fusion Res. SERIES, **9** (2010) 136.
- [3] H. Kawashima, *et al.*: Plasma and Fusion Research: Regular Articles, **1** (2006) 031.
- [4] K. Shimizu, *et al.*: J. Nucl. Mater. **390-391** (2009) 307.
- [5] D. Post, *et al.*: Phys. Plasmas **2** (1995) 2328.
- [6] H. Kawashima, *et al.*: Nucl. Fusion **49** (2009) 065007.